energies

MDPI

Article

The Effect of Multi-Walled Carbon Nanotubes-Additive in Physicochemical Property of Rice Brand Methyl Ester: Optimization Analysis

Fitranto Kusumo [1,2,3,*], T.M.I. Mahlia [4], A.H. Shamsuddin [1], Hwai Chyuan Ong [2,*], A.R Ahmad [3], Z. Ismail [5], Z.C. Ong [2] and A.S. Silitonga [1,6]

1 Institute of Sustainable Energy, Universiti Tenaga Nasional, Kajang 43000, Selangor, Malaysia
2 Department of Mechanical Engineering, Faculty of Engineering, University of Malaya, Kuala Lumpur 50603, Malaysia
3 Department of Computer Science & Information Technology, College of Computer Science & Information Technology Universiti Tenaga Nasional, Kajang 43000, Selangor, Malaysia
4 School of Information, Systems and Modelling, Faculty of Engineering and Information Technology, University of Technology Sydney, Sydney, NSW 2007, Australia
5 Department of Civil Engineering, Faculty of Engineering, University of Malaya, Kuala Lumpur 50603, Malaysia
6 Department of Mechanical Engineering, Politeknik Negeri Medan, Medan 20155, Indonesia
* Correspondence: fitrantokusumo@yahoo.co.id (F.K.); onghc@um.edu.my (H.C.O.)

Received: 11 July 2019; Accepted: 23 August 2019; Published: 26 August 2019

Abstract: Biodiesel as an alternative to diesel fuel produced from vegetable oils or animal fats has attracted more and more attention because it is renewable and environmentally friendly. Compared to conventional diesel fuel, biodiesel has slightly lower performance in engine combustion due to the lower calorific value that leads to lower power generated. This study investigates the effect of multi-walled carbon nanotubes (MWCNTs) as an additive to the rice bran methyl ester (RBME). Artificial neural network (ANN) and response surface methodology (RSM) was used for predicting the calorific value. The interaction effects of parameters such as dosage of MWCNTs, size of MWCNTs and reaction time on the calorific value of RBME were studied. Comparison of RSM and ANN performance was evaluated based on the correlation coefficient (R^2), the root mean square error (RMSE), the mean absolute percentage error (MAPE), and the average absolute deviation (AAD) showed that the ANN model had better performance (R^2 = 0.9808, RMSE = 0.0164, MAPE = 0.0017, AAD = 0.173) compare to RSM (R^2 = 0.9746, RMSE = 0.0170, MAPE = 0.0028, AAD = 0.279). The optimum predicted of RBME calorific value that is generated using the cuckoo search (CS) via lévy flight optimization algorithm is 41.78 (MJ/kg). The optimum value was obtained using 64 ppm of < 7 nm MWCNTs blending for 60 min. The predicted calorific value was validated experimentally as 41.05 MJ/kg. Furthermore, the experimental results have shown that the addition of MWCNTs was significantly increased the calorific value from 36.87 MJ/kg to 41.05 MJ/kg (11.6%). Also, the addition of MWCNTs decreased flashpoint (−18.3%) and acid value (−0.52%). As a conclusion, adding MWCNTs as an additive had improved the physicochemical properties characteristics of RBME. To our best knowledge, no research has yet been performed on the effect of multi-walled carbon nanotubes-additive in physicochemical property of rice brand methyl ester application so far.

Keywords: optimization; rice bran biodiesel; multi-walled carbon nanotube; additive; response surface methodology; artificial neural network; alternative fuel

1. Introduction

In the present day, fossil fuel resources are depleting and become in a critical stage. The increasing consumption of this fossil fuel has a negative impact on the environment and climate [1]. This condition led researchers to develop alternative fuels to reduce the air pollution caused by increasing consumption of this fossil fuel. There are many types of renewable energy sources have been developed, such as solar, wind, biofuel, and geothermal [2–6]. However, the problem of most of the renewable energy like solar and wind is energy storage since the availability is only for a specific time and unstable [7,8]. Therefore, the energy coming from agricultural waste and non-edible is still the best choices. Among the various alternative fuels, biodiesel is the most desirable fuel that can be used in current diesel engines [9–16]. Biodiesel is biodegradable, non-toxic, and environmentally-friendly fuel due to biodiesel produced by transesterification from renewable resources [17–24].

However, the disadvantages of biodiesel fuels derived from vegetable oils have lower calorific value compared to diesel fuel due to the lower carbon-oxygen ratio that makes the excess of oxygen in biodiesel fuels [25,26]. This condition will lead to lower power generated, and thus increasing the fuel consumption for the same amount of power generated from a diesel engine. To overcome this disadvantage, many researchers study the potential of nanoparticles such as carbon nanotubes (CNT) as an additive to improve the quality and fuel properties [27–30]

CNT is a pure carbon substance built in a cylindrical shape in nanometre size multi-surface materials which has properties such as high surface area, excellent stiffness, and durability which have been used for numerous engineering applications. Using the CNT in diesel-biodiesel blends will increase the ratio of carbon-oxygen, thus improving the burning rate of the fuel, the cetane number acts as an antiknock additive and reduced harmful pollutants [24,25].

Basha and Anand [31] reported in their studies that adding the CNT as an additive increased the calorific value about 2.31% from 38.88 to 39.78 (MJ/kg). Ahmad et al. [27] investigated the effect of Carbon Nanotubes (CNT) as an additive to the palm biodiesel. Multiwall carbon nanotubes (MWCNTs) with a size of 10–20 nm and the particle length in between 10–30 μm disperses with Scientz ultrasonic for 40 minutes in the palm biodiesel. The results reported that dispersing maximum CNT concentration increase the calorific value by 1.4% from 52.0 to 52.7 MJ/kg of the palm biodiesel. Balaji and Cheralathan [28] use Carbon Nanotubes (CNT) as an additive in neem oil biodiesel, and the result has shown that adding CNT as additive increased of calorific value by 0.62%.

Carbon nanotubes (CNT) are characterized as a graphene sheet rolled-up to form a tube. Carbon nanotubes are categorized as multi-walled nanotubes (MWCNTs) or single-walled nanotubes (SWCNTs). MWCNTs are cheaper to produce and have better dispersion compared to SWCNTs [32,33]. It is undeniable that the cost of preparing carbon nanotube materials is higher than metal oxides. Therefore, the researcher is still in search for new sources (i.e., natural hydrocarbon precursors, waste materials, and food products) and production method (i.e., arc discharge, laser evaporation/ablation, chemical vapour deposition) of carbon that are cost-effective, so that the price of CNTs can be reduced to an appropriate level [34,35].

Owing to the above potential effect of the CNT in improving the properties of biodiesel, therefore, the aim of this study is to optimize the calorific value of rice bran methyl ester (RBME) by blending with MWCNTs as additive using the artificial neural network (ANN) and response surface methodology (RSM) as optimization methods.

One the most effective optimization method is Response surface methodology (RSM), which correlate the relationship between parameters in the experimental and the result. The effect of independent variables is determined by RSM and also created a mathematical model. Therefore, many researchers have studied and developed the model of biodiesel production using RSM to improve biodiesel quality. In this study, RSM is a mathematical modelling used to develop an empirical model and to perform optimization [36], whereas the artificial neural network is a soft computing technique which imitates the biological processing ability of the human brain [37,38]. Artificial neural networks have been applied in numerous studies due to its capability to handle modelling and simulation of

complex nonlinear systems [39–41]. However, several references reported that artificial neural networks have better performance in prediction effectiveness compare to response surface methodology [42,43]. Cuckoo search optimization algorithm (CS) via *lévy* flight is a stochastic global search metaheuristic technique that inspired by the brood parasitism of some cuckoo species combining with the *lévy* flight that inspired by the flight behaviour of fruit flies [44]. Coupling cuckoo search optimization algorithm via *lévy* flight with the artificial neural network is desirable since the cuckoo search optimization algorithm via *lévy* flight is capable of optimizing complex process parameters [45].

Therefore, this present work, aimed at to compare the response surface methodology (RSM) and artificial neural network (ANN) model for the process of predicting and optimizing the calorific value of rice bran methyl ester by adding multi-walled carbon nanotubes (MWCNTs) as additive. The cuckoo search (CS) optimization algorithm via *lévy* flight is selected to optimize the ANN model. Furthermore, properties such as flash point, acid value, oxidation stability, kinematic viscosity, and density were also investigated. Based on the literature survey, there is no publication has been investigated on the effect of multi-walled carbon nanotubes-additive in physicochemical property of rice brand methyl ester application at the moment.

2. Materials and Methods

2.1. Materials

Rice bran crude oil was purchased in Kuala Lumpur, Malaysia. The reagents used during the biodiesel process production were methanol (purity: 99.9%), potassium hydroxide pellets (KOH). Whatman filter papers (Filtres Fioroni, France) were purchased from local suppliers. Multi-walled carbon nanotubes (WCNTs) size < 7, 20–30 and 50–80 nm were purchased from Merck Sdn. Bhd., Malaysia.

2.2. Experimental Setup

The research found that the rice bran oil acid value is below 2 mg KOH/g and therefore, the acid-catalyzed esterification was not conducted. However, the rice bran oil transesterification process was conducted by a 1000 ml double jacketed reactor. The reactor used equipped with a reflux condenser, thermometer and an overhead stirrer fitted with a digital speed indicator (Model: IKA®RW 16, IKA-Werke GmbH & Co. KG, Germany) to control the temperature. The regulator was used to make sure proper mixing occurred in the reaction mixture. The reaction system was controlled using a water circulator in the reactor vessel outer wall. The equipment used for this purpose was WiseCircu®precise digital refrigerated bath circulator (Model: WCR-P8, Daihan Scientific, South Korea) and this is monitored using a thermometer. The experiment setup of biodiesel production is illustrated in Figure 1a.

Beakers of 500 ml capacity made of borosilicate glass and aluminium foil were used for the mixing the RBME and multi-walled carbon nanotubes (MWCNTs). The ultrasound equipment (Model: Qsonicav (Q500-20)) with a 1/2″ probe and operating at a frequency of 20 kHz and fixed power dissipation of 120 W was used as a particle homogenization device. The device supply the sound wave that contained high energy to multi-walled carbon nanotubes (MWCNTs) blend mixtures with rice bran methyl ester (RBME). The experiment setup of homogenizer of RBME and MWCNTs is illustrated in Figure 1b.

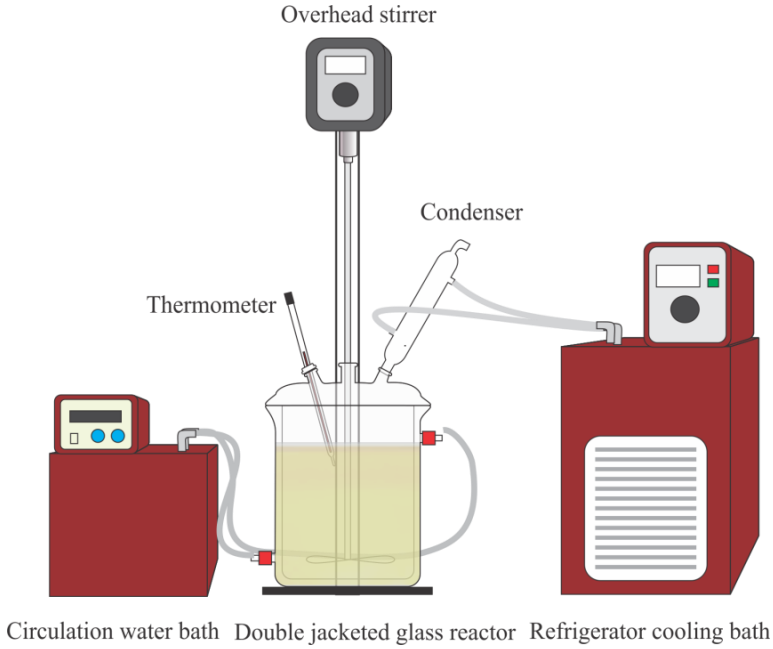

(**a**)

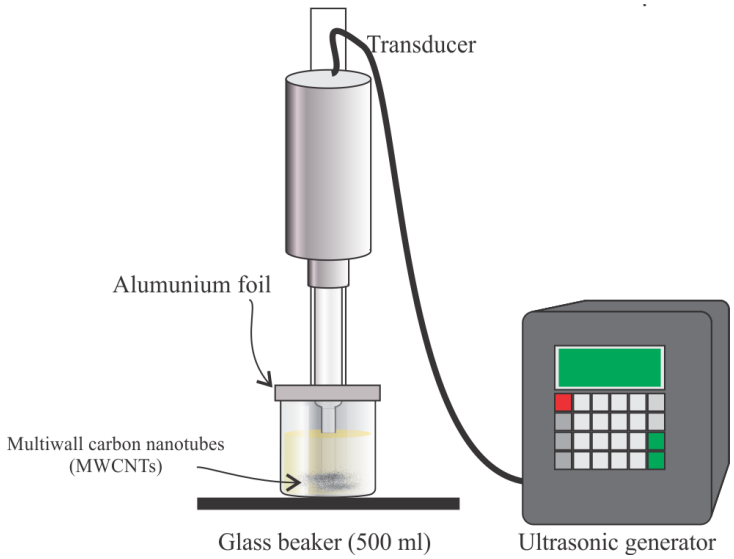

(**b**)

Figure 1. (**a**). Biodiesel production using ultrasound equipment system; (**b**) ultrasound homogenization device.

2.3. Methods

2.3.1. Rice Bran Biodiesel Production

Alkaline-catalyzed transesterification for the biodiesel conversion process is suitable to use if the acid value of oil is less than 2 mg KOH/g [46]. In this study, one step biodiesel production process (alkaline-catalyzed transesterification) was conducted, as the rice bran crude oil acid value is below 2 mg KOH/g (1.8 mg KOH/g). The optimize parameter for the alkaline-catalyzed transesterification for rice bran oil were: KOH 0.9% w/w, with methanol molar ratio 6:1, reaction temperature 60 °C,

and reaction time 60 min with 1000 rpm stirring speed [47]. When the reaction is finished, the biodiesel in this case methyl ester was dispensed for 6 h in a separating funnel. The purpose of this experiment is to make methyl ester and glycerol separated. The glycerol, methanol surplus and impurities in the experiment usually having higher density and must be removed at this stage from most bottom layer. Subsequently, the methyl ester was discharged to rotary evaporator to separate residues of methanol. The process then followed by using distilled water to wash several times, this is to separate entrained glycerol and impurities of the sample. In this experiment the 50% (v/v) of distilled water around 50 °C was sprayed on the methyl ester surface and slowly then stirred. This methyl ester, then vacuum pump used to purify further to separate surplus water and methanol at the temperature 60 °C, and lastly filter paper was used to filter the sample.

2.3.2. Blending Multi-Walled Rice Bran Methyl Ester (RBME) with Multi-Walled Carbon Nanotubes (WCNTs) Process

Multi-walled carbon nanotubes (MWCNTs) with varied sizes from >7 to 80 nm are weighed using an electronic weighing balance with high precision to a predetermined mass fraction of 30–90 ppm and blended in rice bran methyl ester (RBME) using ultrasound for 60 min. The schematic diagram of the complete RBME production and blending process of RBME and MWCNTs is presented in Figure 2.

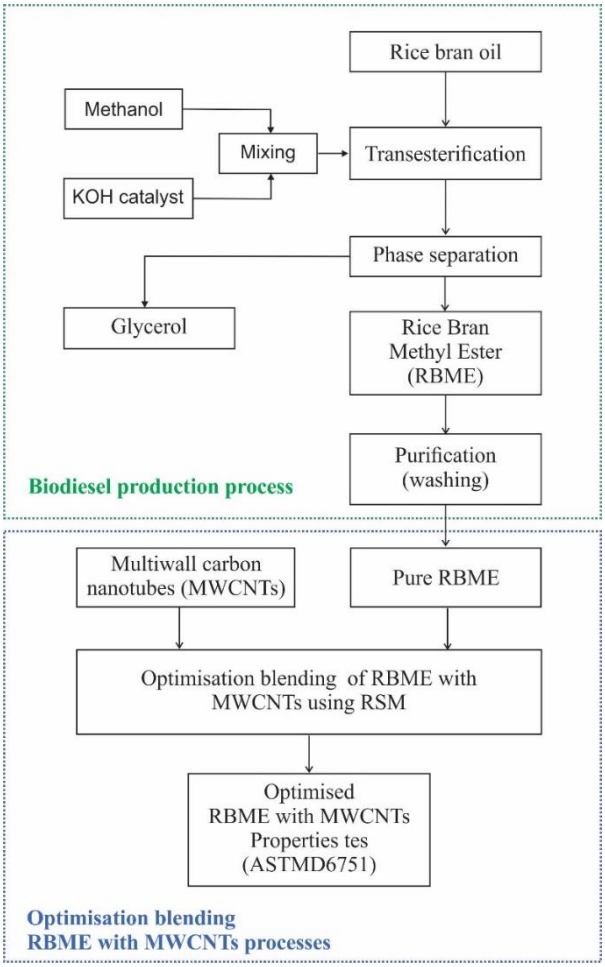

Figure 2. Flow chart of rice bran methyl ester (RBME) production and blending process of RBME and multi-walled carbon nanotubes (MWCNTs).

2.3.3. Properties of Crude Oil and Fatty Acid Composition Analysis

The RBME and RBME essential physicochemical properties with MWCNTs include, flashpoint, density, viscosity, acid value and oxidation stability were determined. The equipment, called Stabinger ViscometerTMSVM 3000 to determine viscosity. The DM40 LiquiPhysicsTM was used to determine the density while calorific value was determined using the 6100EF semi-auto bomb calorimeter (Perry, GA, USA), automation titration Rondo 20 was used to determine the acid value. The Pensky-Martens automatic NPM 440 to determine the flashpoint, and oxidation stability determined by using 873 Biodiesel Rancimat (Metrohm, Switzerland).

2.4. Response Surface Methodology (RSM) is Modelling Optimization of Calorific Value

The process of analyzing and optimizing data of the experiments was performed using analysis of variance (ANOVA) and response surface methodology (RSM) provided by Design-Expert software version 11 (Stat-Ease Inc., Minneapolis, USA). Box–Behnken experimental design was applied to analyze and optimize data of the blending rice bran methyl ester (RBME) with multi-walled carbon nanotubes (MWCNTs). The operating parameters, i.e., the dosage of MWCNTs (X_1), size of MWCNTs (X_2) and reaction time (X_3), were varied in order to optimize the calorific value of RBME blending with MWCNTs (Y). The coded and uncoded levels of the Box–Behnken independent variables were presented in Table 1. Whereas the 17 experimental runs generate using Box–Behnken is listed in Table 2. The experimental data were analyzed in the form of a mathematical model as follows:

$$Y = b_o + \sum_{i=1}^{k} b_i X_i + \sum_{i=1}^{k} b_{ii} X_i^2 + \sum_{i_{i>j}}^{k} \cdot \sum_{j}^{k} b_{ij} X_i X_j + e \quad (1)$$

Table 1. Box–Behnken coded and uncoded independent variables for optimization of the blending process parameters for the *rice bran* methyl ester (RBME) blending with multi-walled carbon nanotubes (MWCNTs).

Parameters	Unit	Coded Variables	Coded Factor Levels		
			−1	**0**	**1**
Dosage of MWCNTs	ppm	x_1	30	60	90
Size of MWCNTs	nm	x_2	< 7	20–30	50–80
Reaction Time	min	x_3	30	45	60

Table 2. Experimental design for optimization of the process parameters for the blending *ricebran* methyl ester (RBME) with multi-walled carbon nanotubes (MWCNTs).

No. of Run	Dosage of MWCNTs (ppm)	Size of MWCNTs (nm)	Time (min)	Calorific Value Experiments (MJ/kg)		
				Experiment	RSM Prediction	ANN Prediction
1	30	50–80	45	38.24	38.32	37.87
2	30	<7	45	39.77	39.62	39.73
3	60	20-30	45	39.78	40.01	40.08
4	60	<7	30	38.77	39.00	38.94
5	60	50–80	30	38.99	38.99	39.00
6	90	<7	45	39.88	39.81	39.88
7	90	50–80	45	39.68	39.84	39.68
8	60	<7	60	40.29	40.30	40.29
9	60	50–80	60	39.26	39.04	39.26
10	60	20–30	45	39.98	40.01	40.08
11	90	20–30	30	38.17	38.03	38.17
12	30	20–30	30	37.98	37.91	38.00
13	30	20–30	60	37.68	37.84	37.59
14	60	20–30	45	40.07	40.01	40.08
15	90	20–30	60	39.37	39.45	39.37
16	60	20–30	45	40.10	40.01	40.08
17	60	20–30	45	40.09	40.01	40.08

In Equation (1), Y is the calorific value (MJ/kg), b_o, b_i, b_{ii} and b_{ii} are regression coefficients, X_i and X_j are the design parameters, k is the number of factors studied and optimized in the experiment, and e is the experimental error attributed to Y [48].

2.5. Artificial Neural Network

In this study, the data collected by the boxbehnken design and the experimental yield values were used for network training to establish the network model using MATLAB R2013b software. Mean square error (MSE) and the coefficient of correlation (R) were used to evaluate the performance of each neural network. The number of the hidden layer with minimum MSE and maximum R^2 was selected as the desired neural network. All experimental data were divided randomly into a training set (70%); validating set (15%); and testing set (15%). The ANN model was performed using Levenberg–Marquardt (LM) algorithm, hyperbolic tangent sigmoid transfer function (tansig) for the input layers, and pure-linear transfer function (purelin) for the output layers.

2.6. Statistical Analysis

The evaluation of the developed RSM and ANN model's performance in prediction, determined using correlation coefficient (R^2), the root means square error (RMSE), the mean absolute percentage error (MAPE), and the average absolute deviation (AAD). The equations used for statistical analysis are given in Equations (2)–(5).

$$R^2 = 1 - \frac{\sum_{i=1}^{n}\left(y_e - y_p\right)^2}{\sum_{i=1}^{n}\left(y_p - y_{avg}\right)^2} \quad (2)$$

$$RMSE = \sqrt{\frac{1}{n}\sum_{i=1}^{n}\left(y_e - y_p\right)^2} \quad (3)$$

$$MAPE = 100 \times \left|\frac{1}{n}\sum_{i=0}^{n}\frac{\left(y_e - y_p\right)}{y_p}\right| \quad (4)$$

$$AAD = \frac{1}{n}\left(\sum_{i=1}^{n}\left(\frac{\left|\left(y_e - y_p\right)\right|}{y_e}\right)\right) \quad (5)$$

where n is the number of points, y_p is the predicted value, y_e is the actual value, and y_{avg} is the average of the actual values.

2.7. Sensitivity Analysis

The significance input variables were calculated based on the partition of the relationship between the weights used equation by Garson [49]. The proposed equation is can be written as follows:

$$pq = \frac{\sum_{r=1}^{r=M_c}\left(\left|W_{qr}^{pc}\right| / \sum_{d=1}^{M_p}\left|W_{dr}^{pc}\right|\right) \times \left|W_{rs}^{cb}\right|}{\sum_{d=1}^{d=M_p}\left\{\sum_{r=1}^{r=M_c}\left(\left|W_{dr}^{pc}\right| / \sum_{d=1}^{M_p}\left|W_{dr}^{pc}\right|\right) \times \left|W_{rs}^{cb}\right|\right\}} \quad (6)$$

where pq is the relative significance of the qc input variable on the output variable, M_p and M_c is the number of input neurons and hidden neurons, respectively, and W is the connection weight. It shall be noted that the superscript p, b and c represent the input, output and hidden layer, respectively, whereas the subscript d, s and r represents the input, output and hidden neuron, respectively.

2.8. Cuckoo Search Via Lévy Flight

Cuckoo Searching consists of three major rules which are as follows: First, each cuckoo tries to find a nest (randomly) to lay one egg. Second, the best nests with high quality eggs will carry over to the next generations [44]. Third, the number of obtainable host nests is fixed and if the egg laid by the cuckoo is discovered by the host bird with a probability of $pa \in [0, 1]$. In this case, the host bird can either throw the egg away or build a new nest in a new location. The last strategy is approximated by a fraction pa of the 'n' nests being replaced by new nests. For generating the new solutions *lévy* flight algorithm is performed according to the following equation [45]:

$$X_i^{(t+1)} = X_i^{(t)} + \hat{\alpha} levy(\lambda) \quad (7)$$

where ($\alpha > 0$) is the step size which is adjusted according to the scale of the problem of interest. The random step length follows the Levy distribution, which has an infinite variance with an infinite mean [24]:

$$levy \sim u = t^{-\lambda}, \; where \; 1 < \lambda \leq 3 \quad (8)$$

2.9. Physicochemical Properties

The 6100EF semi-auto bomb calorimeter was used to determine the calorific value (Perry, GA, USA). The other physicochemical properties of rice bran Methyl Ester (RBME) (i.e., kinematic viscosity, density, flash point, oxidation stability, etc), were determined according to ASTM standard. The result of RBME physicochemical properties compared with the RBME blending with multi-walled carbon nanotubes (MWCNTs) produced from optimum conditions. The physical and chemical properties of the crude *rice bran* crude oil (RBO) in Table 3.

Table 3. Physical and chemical properties of the crude *rice bran* crude oil (RBO).

Properties	*Rice Bran* Crude Oil
Viscosity at 40 °C (mm^2/s)	38.195
Density at 15 °C (kg/m^3)	922.6
Acid number (mg KOH/g)	1.82
Calorific value (MJ/k g)	36.87

3. Results and Discussion

3.1. Modelling and Optimisation by Response Surface Methodology (RSM)

In this study, the quadratic model was selected due to possessing a high significance order, and it is not aliased among the models which were indicated by the software (Table 4). The model used in this equation using a notation such as X_1 for the dosage of multi-walled carbon nanotubes (MWCNTs), X_2 for the size of MWCNTs, and X_3 for the reaction time. The model is shown in the following equation:

$$Y = 29.49992 + 0.072798X_1 - 0.01489X_2 + 0.35112\,X_3 + 0.00030408\,X_1X_2 + 0.0008293889X_1X_3 \\ -0.0005691X_2X_3 - 0.000908125X_1^2 + 0.000155667X_2^2 + -0.00392938889\,X_3^2 \quad (9)$$

The values of the coefficients and the analysis of variance (ANOVA) were presented in Table 5. According to Table 5, the t p-value of the model is < 0.0001 indicated that the model was statistically significant at 95% confidence level for the model term [50]. The parameters (dosage of MWCNTs (X_1), reaction time (X_3) and size of MWCNTs (X_2)) have a significant influence on calorific value response due to the p-values < 0.0500 (46) [51] (Table 5). The lack of fit with a p-value of 0.1069 means the model very well represent the experimental data in the chosen interval.

Table 4. Sequential model sum of squares.

Source	Sum of Squares	df	Mean Square	F Value	*p*-Value Prob> F	Remarks
Mean	26262.64	1	26262.64	-	-	-
Linear	3.21	3	1.07	1.7	0.2161	-
2FI	1.39	3	0.46	0.68	0.5827	-
Quadratic	6.5	3	2.17	52.51	< 0.0001	Suggested
Cubic	0.22	3	0.072	4	0.107	Aliased
Residual	0.072	4	0.018	-	-	-

Table 5. Analysis of variance (ANOVA) for the regression model.

Source	Sum of Squares	df	Mean Square	*F* Value	*p*-value Prob > F[a,b]	Marks
Model	11.0906	9	1.2323	29.8829	<0.0001	significant
X_1-dosage	1.4875	1	1.4875	36.0711	0.0005	-
X_2-size	0.8085	1	0.8085	19.6057	0.0031	-
X_3-time	0.9098	1	0.9097	22.0618	0.0022	-
X_1 X_2	0.4435	1	0.4435	10.7546	0.0135	-
X_1 X_3	0.5572	1	0.5572	13.5118	0.0079	-
X_2 X_3	0.3883	1	0.3883	9.4167	0.0181	-
X_1^2	2.8126	1	2.8126	68.2062	<0.0001	-
X_2^2	0.1811	1	0.1811	4.3915	0.0744	-
X_3^2	3.2912	1	3.2912	79.8109	<0.0001	-
Residual	0.2887	7	0.0412	-	-	-
Lack of Fit	0.2165	3	0.0722	3.9981	0.1069	not significant

[a] Significant at "Prob > F" lower than 0.05; [b] Insignificant at "Prob > F" higher than 0.1.

From the Figure 3, the value of R^2 is 0.974 indicated the model with 97.46% of variability, which meant that the model has an acceptable level for the model accuracy (R^2 value close to unity).

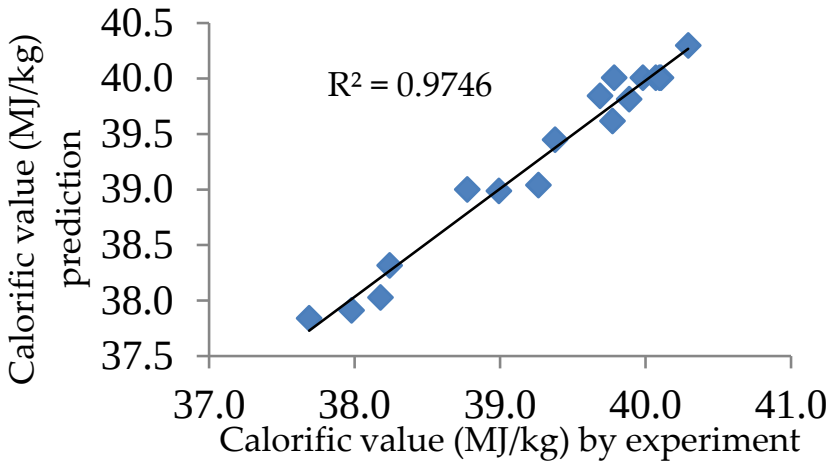

Figure 3. The plot of the experimental versus predicted *rice bran* methyl ester (RBME) blending with multi-walled carbon nanotubes (MWCNTs) calorific value using RSM.

The deviation between the predicted values against the actual value was determined to validate the adequacy of the model. Figure 4a shows that the errors are distributed normally in a straight line, whereas the residuals versus predicted response shown in Figure 4b. The figure shows that the points are scattered randomly in the plot, indicating that the model is adequate.

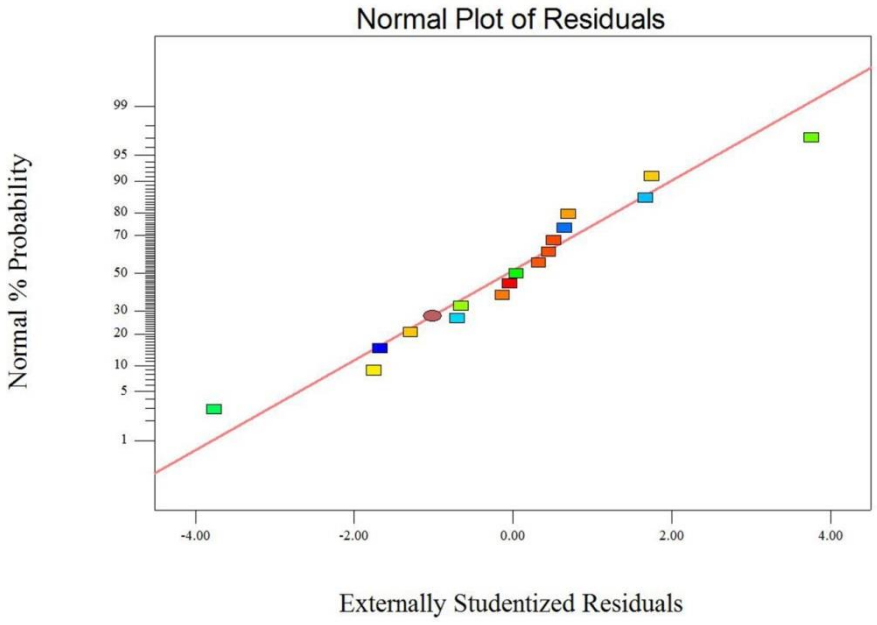

(**a**)

Figure 4. *Cont*.

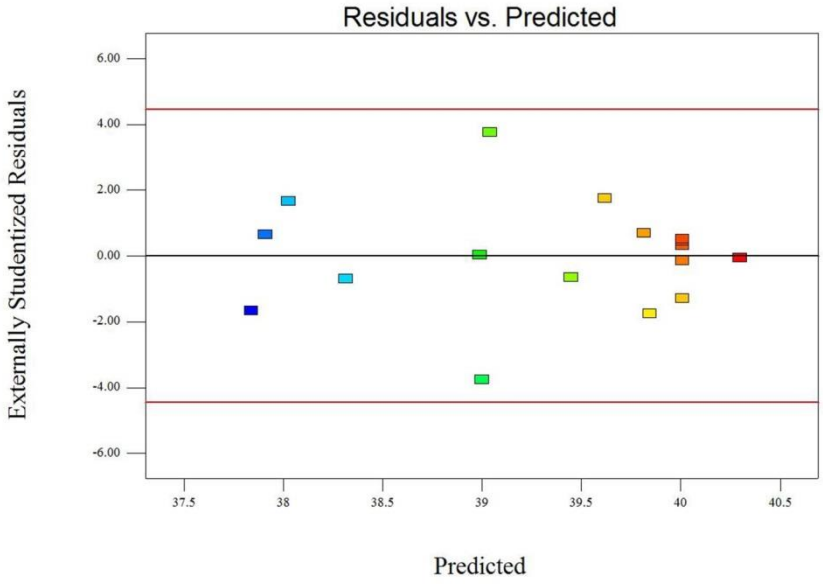

(**b**)

Figure 4. (**a**) Normal probability plots of the residuals and; (**b**) plot of the residuals versus the predicted response.

3.2. *Effect of the Parameter*

A response surface plot for blending rice bran methyl ester (RBME) with multi-walled carbon nanotubes (MWCNTs) presented in Figure 5. The interaction of MWCNTs size and dosage of MWCNTs to the calorific values illustrated Figure 5a. The p-value of his interaction was 0.0135 (Table 5). From the figure, it could be seen that the calorific value was strongly influenced by the variation of MWCNTs dosage. The calorific value was increased significantly from 30–63 ppm of MWCNTs dose and then decreasing gradually. On the contrary, the increasing size of MWCNTs leads the decreasing the calorific value of RBME. This occurs because the bigger size of the MWCNTs cannot disperse completely on RBME. The properties improvement of biodiesel using nanoparticle as additive depending upon the size of nanoparticles [52].

Figure 5b, illustrated the interaction between reaction time and dosage of MWCNTs. The p-value = 0.0079 of the interaction between reaction time and dosage of MWCNTs indicated that there was a relatively significant (Table 5). The significant interaction is proven by the elliptical 3D contours from the interaction between reaction time and dosage of MWCNTs (Figure 5b) and their effects on the calorific value of RBME. The calorific value increased with the increasing of the reaction time from 30–50 min followed by the increasing dosage of MWCNTs from 30–63 ppm, which could be attributed to the reason that more dosage of MWCNTs creates a more active reaction. The calorific values were decreasing when the dosage of MWCNTs reached above 63 ppm with reaction time more than 50 min. However, further higher reaction time and dosage of MWCNTs lead the decreasing of the calorific value. This is due to the excess carbon present in the fuel at higher dosages and reaction time caused the ratio of carbon to oxygen to be saturated. Adding MWCNTs beyond this saturation point will not enhance the combustion capability of the fuel further.

The interaction of reaction time and the size of MWCNTs presented in Figure 5c, with the p = value of the interactions is 0.0181. From the figure, it can be seen that the calorific value increased with increasing reaction time from 30 to 50 min. On the other hand, the larger size of MWCNTs leads to the decreasing of RBME calorific value.

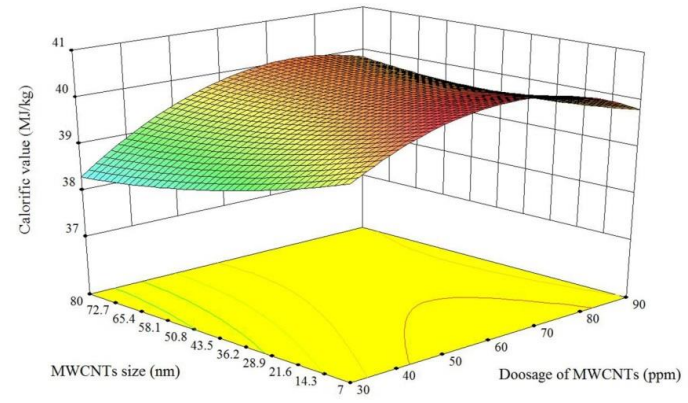

(**a**)

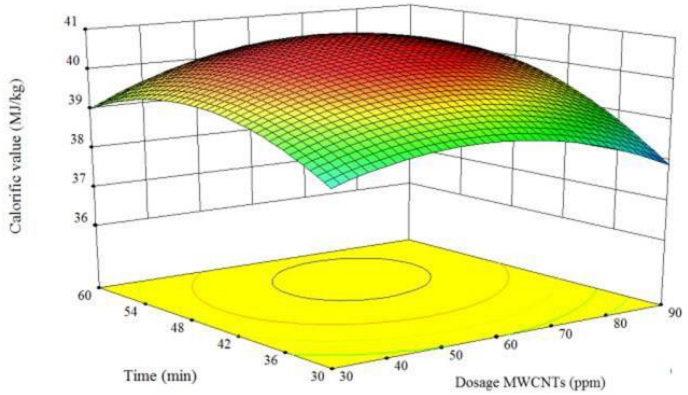

(**b**)

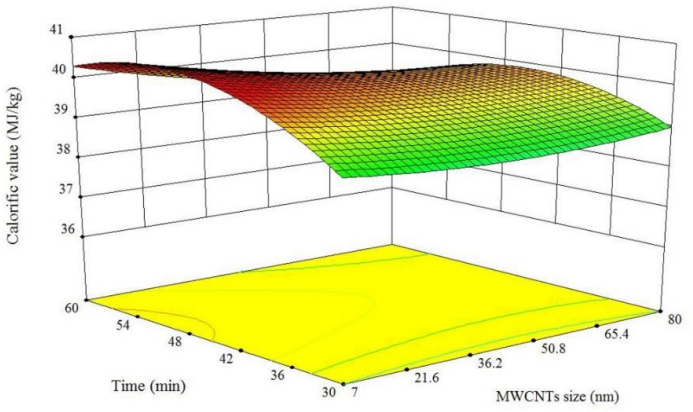

(**c**)

Figure 5. The three-dimensional surface plot which shows the combined effects of: (**a**) time and multi-walled carbon nanotubes (MWCNTs) size; (**b**) time and dosage MWCNTs; (**c**) time and MWCNTs size.

3.3. Artificial Neural Network

The prediction of rice bran calorific value was calculated by ANN with Levenberg–Marquardt backpropagation algorithm. a total of 17 experimental were conducted using three input parameters (i.e., dosage of MWCNTs, Size of MWCNTs, and time) and calorific value as output variable (Table 2).

The optimum number of hidden neurons was trained based on the minimum mean square error (MSE) and the maximum value of correlation coefficient (R). The best topology in this study was found to be 3–5–1, (Figure 6). Correlation coefficient (R) plots for the training, testing, validation, and whole datasets are given in Figure 7. The value of R^2 (Figure 8) is 0.9809 indicated the model with 98.09% of variability, which meant that the model has an acceptable level for the model accuracy.

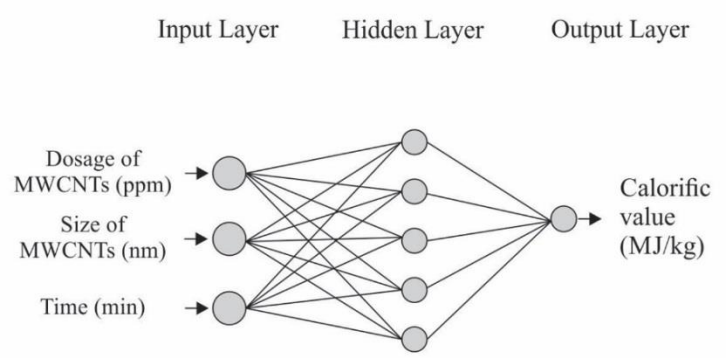

Figure 6. Typical architecture of artificial neural network (ANN).

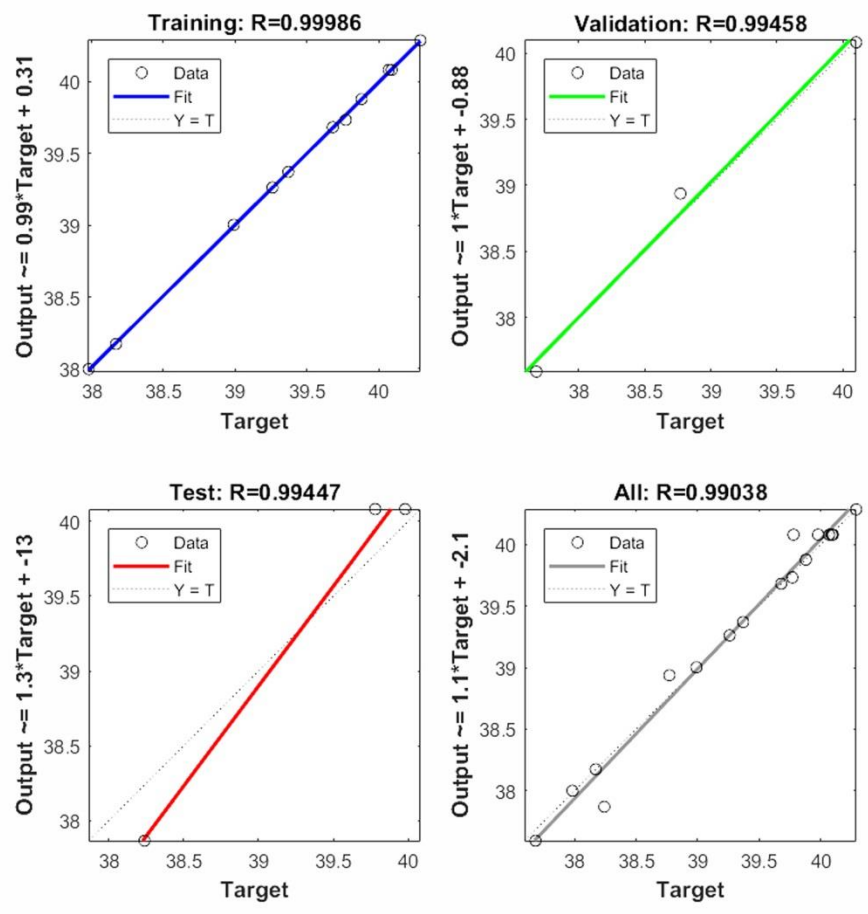

Figure 7. Neural network models with training, validation, test, and all prediction set.

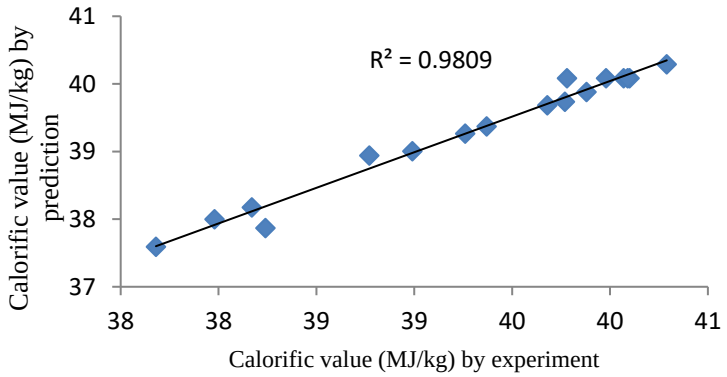

Figure 8. The plot of the experimental versus predicted *rice bran* methyl ester (RBME) blending with multi-walled carbon nanotubes (MWCNTs) calorific value using artificial neural network (ANN).

3.4. Performance Assessment of Response Surface Methodology (RSM) and Artificial Neural Network (ANN)

The performance of the RSM and ANN models were statistically measured by determining their correlation coefficient (R^2), the root means square error (RMSE), the mean absolute percentage error (MAPE), and the average absolute deviation (AAD). The calculation results are tabulated in Table 6. Both ANN and RSM had high values of R^2, indicating that the models are in a good fit. The RSM prediction has a slightly higher deviation with the value of RMSE = 0.0170 than ANN (0.0164). The AAD for RSM and ANN was found to be 0.173 and 0.279. MAPE was to measure the accuracy and precision of both RSM and ANN. Based on the statistical results, it could be concluded that the ANN model was better than the RSM model due to the lower values for RSME, MAPE, ADD, and the higher value of R^2.

Table 6. Comparison of statistical criteria of models.

Parameter	RSM	ANN
R^2	0.9746	0.9809
RMSE	0.0170	0.0164
MAPE	0.0028	0.0017
AAD	0.279	0.173

3.5. Optimisation and Sensitivity Analysis

The ANN model coupled with a cuckoo search via *lévy* flight optimization algorithm was used to generate the optimal condition values of operating parameters. The optimum calorific value 41.78 MJ/kg was achieved with a dosage of MWCNTs 64 ppm, < 7 nm size of MWCNTs blending for 60 minutes, which was validated by experimental results as 41.05 MJ/kg.

Figure 9 illustrated the impact of the parameters (Dosage of MWCNTs, Size of MWCNTs, and time) on the blending MWCNTs in rice bran methyl ester. The higher value for the Size of MWCNTs (44.04%) indicates that parameter had a more impact on the optimizing calorific value on the rice bran methyl ester followed by a dosage of MWCNTs (37.15%) and time (18.81%).

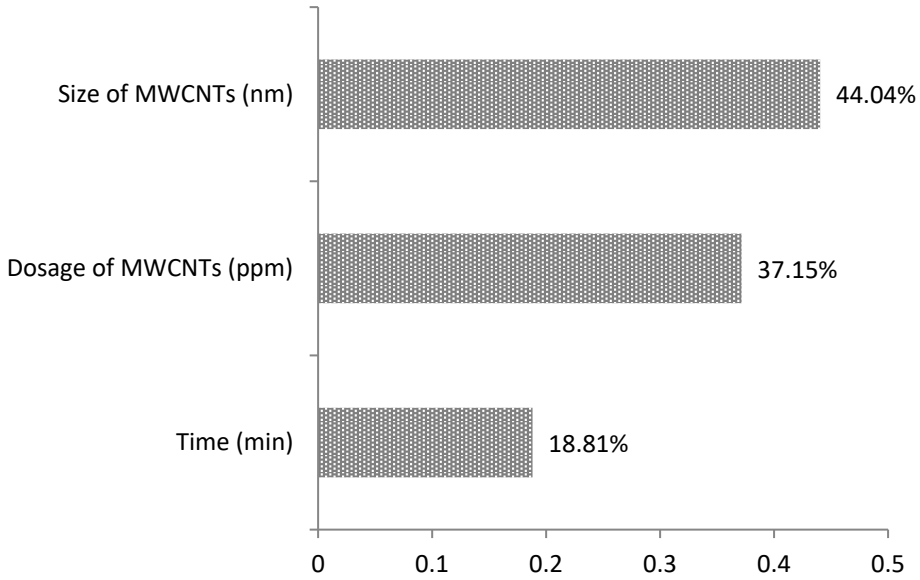

Figure 9. Sensitivity analysis of parameter.

3.6. Physicochemical Properties of Rice Bran Methyl Ester (RBME) and RBME with Multi-Walled Carbon Nanotubes (MWCNTs) in Optimum Condition

The comparison of rice bran methyl ester (RBME) physicochemical properties compared with RBME blending with multi-walled carbon nanotubes (MWCNTs) after optimization are presented in Table 7. The addition MWCNTs blending with biodiesel was able to improve the characteristics, such as the calorific value. The calorific value is one of the essential properties, since the higher the calorific value of a fuel, the higher its combustion rate is. The investigation of the calorific value of RBME blending with MWCNTs after optimization will determine the compatibility of the fuel to be adopted in the existing CI engines without significant adjustment required to the engine. The calorific value of RBME before adding MWCNTs was 37.44 MJ/kg, due to its high oxygen content in the fuel. The calorific values of RBME significantly increase to 41.05 MJ/kg after adding MWCNTs as additive. The optimum calorific value of RBME after adding MWCNTs as additive achieved at a dosage of MWCNTs 64 ppm, < 7 nm size of MWCNTs blending in 60 minutes. Furthermore, adding MWCNTs at optimum condition decreasing 18.13 % the flashpoint from 185 °C to 152 °C. This could be due to the characteristic of WCNT that have a high surface area and reactive surfaces, which could contribute to higher chemical reactivity that can enhance higher carbon combustion activation [53]. The acid value of the RBME blending with MWCNTs is found to be 0.08 mg KOH/g, decreasing from 0.17 mg KOH/g. The oxidation stability of adding MWCNTs in RBME also increased from 4.89 h to 5.01 h. The same goes for the kinematic viscosity and density, by adding MWCNTs to RBME, the values are slightly increased from 4.801 to 4.895 mm^2/s and 879.2 to 879.8 kg/m^3, respectively. This is in line with experimental results by Banapurmath et al., and Tewari et al., they reported that by the addition of nanoparticles, the biodiesel viscosity properties were increased [54,55]. However, the increase of kinematic viscosity and density still in the range of ASTM 6751 standard.

Table 7. Physical and chemical properties of the pure *rice bran* methyl ester (RBME) and RBME with multi-walled carbon nanotubes (MWCNTs).

Properties	Unit	Standard Test Method	ASTM D6751	Diesel	RBME	*RBME with* MWCNTs	*Improvement*
Viscosity at 40 °C	mm^2/s	D 445	1.9 6.0	2.86	4.801 ± 0.1	4.895 ± 0.3	1.96%
Density at 15 °C	kg/m^3	D 1298	860 880	833	879.2 ± 1.4	879.8 ± 1.2	0.07%
Acid number	mg KOH/g	D 664	Max. 0.5	0.06	0.17 ± 1.4	0.08 ± 1.3	−52.94%
Flash point	°C	D 93	Min. 130	70.5	185 ± 3.6	152 ± 3.7	−17.84%
Calorific value	MJ/kg	D 975	Min. 35	45.82	37.44 + 0.3	41.05 ± 0.1	9.64%
Oxidation stability at 110 °C	h	EN 14112	Max. 3	15.2	4.89 ± 0.1	5.01 ± 0.5	2.45%

4. Conclusions

In the present study, experimental work on blending rice bran methyl ester (RBME) with multi-walled carbon nanotubes (MWCNTs) was carried out. The main purpose of this study is to optimize the calorific value and to find the effects dosage of MWCNTs, size of MWCNTs, and reaction time using RSM and ANN on rice band methyl ester. The predictive capability of the ANN and RSM models was compared using statistical criteria, i.e., R^2, RMSE, MAPE, and AAD. The ANN model has higher R^2 (0.9809) compared to the RSM model and the value of RMSE, MAPE, and AAD are smaller than the RSM model. From the results, it is shown that the ANN model was more accurate than the RSM model.

The optimum calorific value was 64 ppm of MWCNTs dosage, < 7 nm of MWCNTs blending for 60 minutes, 41.78 MJ/kg was obtained at optimum condition generated using cuckoo search via *lévy* flight optimization algorithm and was validated by experimental results as 41.05 MJ/kg. The study also revealed that the size of MWCNTs had a significant influence, followed by a dosage of MWCNTs and reaction in the blending process.

The addition of MWCNTs significantly improves some properties of RBME, such as flash point, acid value, and calorific value. The flashpoint value decreases 17.84% from 185 °C to 152 °C while for acid value, there have significantly decreased from 0.17 to 0.08 mg KOH/g (52.94%.), while for the calorific value, increment reaches 9.64% from 37.44 to 41.05 MJ/kg. However, the addition of MWCNTs turned out to slightly decrease (< 5%) the kinematic viscosity and density for 1.96% and 0.07%, respectively.

Author Contributions: Conceptualization, Methodology, results and formal analysis were initiated and wrote by F. Kusumo, T.M.I. Mahlia, and Hwai Chyuan Ong; A.H. Shamsuddin and A.R. Ahmad contributed to the Mathematical derivation and results analysis; Z. Ismail and Z.C. Ong checked and improved the manuscript. All authors read and approved the final manuscript.

Funding: This research is funded by the Centre for Advanced Modeling and Geospatial Information Systems (CAMGIS), UTS under Grants 321740.2232397 and AAIBE Chair of Renewable grant no: 201801 KETTHA. The authors would like to acknowledge the University of Malaya, Kuala Lumpur for the financial support under SATU joint research scheme (ST010-2018), the Direktorat Jenderal Penguatan Riset dan Pengembangan Kementerian Riset, Teknologi dan Pendidikan Tinggi Republik Indonesia, (Grant no. 147/SP2H/LT/ DRPM/2019) and Politeknik Negeri Medan, Medan, Indonesia

Conflicts of Interest: The authors declare no conflict of interest.

References

1. Norhasyima, R.S.; Mahlia, T.M.I. Advances in CO2 utilization technology: a patent landscape review. *J. CO2 Util.* **2018**, *26*, 323–335. [CrossRef]
2. Alhamid, M.I.; Daud, Y.; Surachman, A.; Sugiyono, A.; Aditya, H.B.; Mahlia, T.M. Potential of geothermal energy for electricity generation in Indonesia: a review. *Renew. Sustain. Energy Rev.* **2016**, *53*, 733–740.
3. Ismail, M.S.; Moghavvemi, M.; Mahlia, T.M.I. Characterization of PV panel and global optimization of its model parameters using genetic algorithm. *Energy Convers. Manag.* **2013**, *73*, 10–25. [CrossRef]
4. Uddin, M.N.; Techato, K.; Taweekun, J.; Rahman, M.M.; Rasul, M.G.; Mahlia, T.M.I.; Ashrafur, S.M. an Overview of Recent Developments in Biomass Pyrolysis Technologies. *Energies* **2018**, *11*, 3115. [CrossRef]

5. Ismail, M.S.; Moghavvemi, M.; Mahlia, T.M.I. Techno-economic analysis of an optimized photovoltaic and diesel generator hybrid power system for remote houses in a tropical climate. *Energy Convers. Manag.* **2013**, *69*, 163–173. [CrossRef]
6. Mofijur, M.; Hazrat, M.A.; Rasul, M.G.; Mahmudul, H.M. Comparative Evaluation of Edible and Non-edible Oil Methyl Ester Performance in a Vehicular Engine. *Energy Procedia* **2015**, *75*, 37–43. [CrossRef]
7. Mehrali, M.; Latibari, S.T.; Mehrali, M.; Mahlia, T.M.I.; Metselaar, H.S.C.; Naghavi, M.S.; Sadeghinezhad, E.; Akhiani, A.R. Preparation and characterization of palmitic acid/graphene nanoplatelets composite with remarkable thermal conductivity as a novel shape-stabilized phase change material. *Appl. Therm. Eng.* **2013**, *61*, 633–640. [CrossRef]
8. Amin, M.; Putra, N.; Kosasih, E.A.; Prawiro, E.; Luanto, R.A.; Mahlia, T.M.I. Thermal properties of beeswax/graphene phase change material as energy storage for building applications. *Appl. Therm. Eng.* **2017**, *112*, 273–280. [CrossRef]
9. Nasreen, S.; Liu, H.; Skala, D.; Waseem, A.; Wan, L. Preparation of biodiesel from soybean oil using La/Mn oxide catalyst. *Fuel Process. Technol.* **2015**, *131*, 290–296. [CrossRef]
10. Silitonga, A.S.; Masjuki, H.H.; Ong, H.C.; Mahlia, T.M.I.; Kusumo, F. Optimization of extraction of lipid from Isochrysis galbana microalgae species for biodiesel synthesis. *Energy Source. Part a Recovery Util. Environ. Eff.* **2017**, *39*, 1167–1175. [CrossRef]
11. Silitonga, A.S.; Atabani, A.E.; Mahlia, T.M.I.; Masjuki, H.H.; Badruddin, I.A.; Mekhilef, S. a review on prospect of Jatropha curcas for biodiesel in Indonesia. *Renew. Sustain. Energy Rev.* **2011**, *15*, 3733–3756. [CrossRef]
12. Kusumo, F.; Silitonga, A.S.; Ong, H.C.; Masjuki, H.H.; Mahlia, T.M.I. a comparative study of ultrasound and infrared transesterification of Sterculia foetida oil for biodiesel production. *Energy Source. Part A. Recovery Util. Environ. Eff.* **2017**, *39*, 1339–1346. [CrossRef]
13. Dharma, S.; Masjuki, H.H.; Ong, H.C.; Sebayang, A.H.; Silitonga, A.S.; Kusumo, F.; Mahlia, T.M.I. Optimization of biodiesel production process for mixed Jatropha curcas–Ceiba pentandra biodiesel using response surface methodology. *Energy Convers. Manag.* **2016**, *115*, 178–190. [CrossRef]
14. Mazaheri, H.; Ong, H.C.; Masjuki, H.H.; Amini, Z.; Harrison, M.D.; Wang, C.-T.; Kusumo, F.; Alwi, A. Rice bran oil based biodiesel production using calcium oxide catalyst derived from Chicoreus brunneus shell. *Energy* **2018**, *144*, 10–19. [CrossRef]
15. Mofijur, M.; Atabani, A.E.; Masjuki, H.H.; Kalam, M.A.; Masum, B.M. a study on the effects of promising edible and non-edible biodiesel feedstocks on engine performance and emissions production: a comparative evaluation. *Renew. Sustain. Energy Rev.* **2013**, *23*, 391–404. [CrossRef]
16. Mofijur, M.; Masjuki, H.H.; Kalam, M.A.; Hazrat, M.A.; Liaquat, A.M.; Shahabuddin, M.; Varman, M. Prospects of biodiesel from Jatropha in Malaysia. *Renew. Sustain. Energy Rev.* **2012**, *16*, 5007–5020. [CrossRef]
17. Dove, J. Student Teacher Understanding of the Greenhouse Effect, Ozone Layer Depletion and Acid Rain. *Environ. Educ. Res.* **1996**, *2*, 89–100. [CrossRef]
18. Silitonga, A.S.; Masjuki, H.H.; Ong, H.C.; Sebayang, A.H.; Dharma, S.; Kusumo, F.; Siswantoro, J.; Milano, J.; Daud, K.; Mahlia, T.M.I.; et al. Evaluation of the engine performance and exhaust emissions of biodiesel-bioethanol-diesel blends using kernel-based extreme learning machine. *Energy* **2018**, *159*, 1075–1087. [CrossRef]
19. Ong, H.C.; Masjuki, H.H.; Mahlia, T.M.I.; Silitonga, A.S.; Chong, W.T.; Yusaf, T. Engine performance and emissions using Jatropha curcas, Ceiba pentandra and Calophyllum inophyllum biodiesel in a CI diesel engine. *Energy* **2014**, *69*, 427–445. [CrossRef]
20. Silitonga, A.S.; Masjuki, H.H.; Mahlia, T.M.I.; Ong, H.C.; Chong, W.T. Experimental study on performance and exhaust emissions of a diesel engine fuelled with Ceiba pentandra biodiesel blends. *Energy Convers. Manag.* **2013**, *76*, 828–836. [CrossRef]
21. Ong, H.C.; Masjuki, H.H.; Mahlia, T.M.I.; Silitonga, A.S.; Chong, W.T.; Leong, K.Y. Optimization of biodiesel production and engine performance from high free fatty acid Calophyllum inophyllum oil in CI diesel engine. *Energy Convers. Manag.* **2014**, *81*, 30–40. [CrossRef]
22. Goh, B.H.H.; Ong, H.C.; Cheah, M.Y.; Chen, W.-H.; Yu, K.L.; Mahlia, T.M.I. Sustainability of direct biodiesel synthesis from microalgae biomass: a critical review. *Renew. Sustain. Energy Rev.* **2019**, *107*, 59–74. [CrossRef]

23. Silitonga, A.S.; Mahlia, T.M.I.; Kusumo, F.; Dharma, S.; Sebayang, A.H.; Sembiring, R.W.; Shamsuddin, A.H. Intensification of Reutealis trisperma biodiesel production using infrared radiation: Simulation, optimisation and validation. *Renew. Energy* **2019**, *133*, 520–527. [CrossRef]
24. Mofijur, M.; Masjuki, H.H.; Kalam, M.A.; Atabani, A.E. Evaluation of biodiesel blending, engine performance and emissions characteristics of Jatropha curcas methyl ester: Malaysian perspective. *Energy* **2013**, *55*, 879–887. [CrossRef]
25. Mirzajanzadeh, M.; Tabatabaei, M.; Ardjmand, M.; Rashidi, A.; Ghobadian, B.; Barkhi, M.; Pazouki, M. a novel soluble nano-catalysts in diesel–biodiesel fuel blends to improve diesel engines performance and reduce exhaust emissions. *Fuel* **2015**, *139*, 374–382. [CrossRef]
26. Prabu, A.; Anand, R.B. Emission control strategy by adding alumina and cerium oxide nano particle in biodiesel. *J. Energy Inst.* **2016**, *89*, 366–372. [CrossRef]
27. Alias, A.B.; Thegaraju, D.; Sharma, K.V. Effect of Carbon Nanotube Dispersions to the Palm Oil Diesel-Biodiesel Blend Properties. In Proceedings of the International Conference on Mechanical Engineering Research, Kuantan, Pahang, Malaysia, 1–3 July 2013.
28. Balaji, G.; Cheralathan, M. Effect of CNT as additive with biodiesel on the performance and emission characteristics of a DI diesel engine. *Int. J. ChemTech Res.* **2015**, *7*, 1230–1236.
29. Sadhik Basha, J.; Anand, R.B. Performance, emission and combustion characteristics of a diesel engine using Carbon Nanotubes blended Jatropha Methyl Ester Emulsions. *Alex. Eng. J.* **2014**, *53*, 259–273. [CrossRef]
30. Leong, K.Y.; Ku Ahmad, K.Z.; Ong, H.C.; Ghazali, M.J.; Baharum, A. Synthesis and thermal conductivity characteristic of hybrid nanofluids—A review. *Renew. Sustain. Energy Rev.* **2017**, *75*, 868–878. [CrossRef]
31. Basha, J.S.; Anand, R.B. The influence of nano additive blended biodiesel fuels on the working characteristics of a diesel engine. *J. Braz. Soc. Mech. Sci. Eng.* **2013**, *35*, 257–264. [CrossRef]
32. Soleimani, H.; Baig, M.K.; Yahya, N.; Khodapanah, L.; Sabet, M.; Demiral, B.M.R.; Burda, M. Impact of carbon nanotubes based nanofluid on oil recovery efficiency using core flooding. *Results Phys.* **2018**, *9*, 39–48. [CrossRef]
33. Glomstad, B.; Zindler, F.; Jenssen, B.M.; Booth, A.M. Dispersibility and dispersion stability of carbon nanotubes in synthetic aquatic growth media and natural freshwater. *Chemosphere* **2018**, *201*, 269–277. [CrossRef]
34. Abdalla, S.; Al-Marzouki, F.; Al-Ghamdi, A.A.; Abdel-Daiem, A. Different Technical Applications of Carbon Nanotubes. *Nanoscale Res. Lett.* **2015**, *10*, 358. [CrossRef]
35. Kumar, R.; Singh, R.K.; Singh, D.P. Natural and waste hydrocarbon precursors for the synthesis of carbon based nanomaterials: Graphene and CNTs. *Renew. Sustain. Energy Rev.* **2016**, *58*, 976–1006. [CrossRef]
36. Milano, J.; Ong, H.C.; Masjuki, H.H.; Silitonga, A.S.; Chen, W.-H.; Kusumo, F.; Dharma, S.; Sebayang, A.H. Optimization of biodiesel production by microwave irradiation-assisted transesterification for waste cooking oil-Calophyllum inophyllum oil via response surface methodology. *Energy Convers. Manag.* **2018**, *158*, 400–415. [CrossRef]
37. Navamani Kartic, D.; Aditya Narayana, B.C.; Arivazhagan, M. Removal of high concentration of sulfate from pigment industry effluent by chemical precipitation using barium chloride: RSM and ANN modeling approach. *J. Environ. Manag.* **2018**, *206*, 69–76. [CrossRef]
38. Sabilla, S.I.; Sarno, R.; Siswantoro, J. Estimating Gas Concentration using Artificial Neural Network for Electronic Nose. *Procedia Comput. Sci.* **2017**, *124*, 181–188. [CrossRef]
39. Kusumo, F.; Silitonga, A.S.; Masjuki, H.H.; Ong, H.C.; Siswantoro, J.; Mahlia, T.M.I. Optimization of transesterification process for Ceiba pentandra oil: a comparative study between kernel-based extreme learning machine and artificial neural networks. *Energy* **2017**, *134*, 24–34. [CrossRef]
40. Aarathi, V.; Harshita, E.; Nalinashan, A.; Ashok, S.; Prasad, R.K. Synthesis and characterisation of rubber seed oil trans-esterified biodiesel using cement clinker catalysts. *Int. J. Sustain. Energy* **2019**, *38*, 333–347. [CrossRef]
41. Siswantoro, J.; Hilman, M.Y.; Widiasri, M. Computer vision system for egg volume prediction using backpropagation neural network. *IOP Conf. Ser. Mater. Sci. Eng.* **2017**, *273*, 012002. [CrossRef]
42. Avramović, J.M.; Veličković, A.V.; Stamenković, O.S.; Rajković, K.M.; Milić, P.S.; Veljković, V.B. Optimization of sunflower oil ethanolysis catalyzed by calcium oxide: RSM versus ANN-GA. *Energy Convers. Manag.* **2015**, *105*, 1149–1156. [CrossRef]

43. Betiku, E.; Odude, V.O.; Ishola, N.B.; Bamimore, A.; Osunleke, A.S.; Okeleye, A.A. Predictive capability evaluation of RSM, ANFIS and ANN: a case of reduction of high free fatty acid of palm kernel oil via esterification process. *Energy Convers. Manag.* **2016**, *124*, 219–230. [CrossRef]
44. Yang, X.; Suash, D. Cuckoo Search via Lévy flights. In Proceedings of the 2009 World Congress on Nature & Biologically Inspired Computing (NaBIC), Coimbatore, India, 9–11 December 2009; pp. 210–214.
45. Iglesias, A.; Gálvez, A.; Suárez, P.; Shinya, M.; Yoshida, N.; Otero, C.; Manchado, C.; Gomez-Jauregui, V. Cuckoo Search Algorithm with Lévy Flights for Global-Support Parametric Surface Approximation in Reverse Engineering. *Symmetry* **2018**, *10*, 58. [CrossRef]
46. Silitonga, A.S.; Ong, H.C.; Masjuki, H.H.; Mahlia, T.M.I.; Chong, W.T.; Yusaf, T.F. Production of biodiesel from Sterculia foetida and its process optimization. *Fuel* **2013**, *111*, 478–484. [CrossRef]
47. Lin, L.; Ying, D.; Chaitep, S.; Vittayapadung, S. Biodiesel production from crude rice bran oil and properties as fuel. *Appl. Energy* **2009**, *86*, 681–688. [CrossRef]
48. Ogunkunle, O.; Ahmed, N.A. Response surface analysis for optimisation of reaction parameters of biodiesel production from alcoholysis of Parinari polyandra seed oil. *Int. J. Sustain. Energy* **2019**, *38*, 630–648. [CrossRef]
49. Garson, G.D. Interpreting neural-network connection weights. *AI Expert* **1991**, *6*, 46–51.
50. Santos Jr, O.O.; Maruyama, S.A.; Claus, T.; de Souza, N.E.; Matsushita, M.; Visentainer, J.V. a novel response surface methodology optimization of base-catalyzed soybean oil methanolysis. *Fuel* **2013**, *113*, 580–585. [CrossRef]
51. Yücel, Y. Optimization of biocatalytic biodiesel production from pomace oil using response surface methodology. *Fuel Process. Technol.* **2012**, *99*, 97–102. [CrossRef]
52. Shaafi, T.; Sairam, K.; Gopinath, A.; Kumaresan, G.; Velraj, R. Effect of dispersion of various nanoadditives on the performance and emission characteristics of a CI engine fuelled with diesel, biodiesel and blends—A review. *Renew. Sustain. Energy Rev.* **2015**, *49*, 563–573. [CrossRef]
53. El-Seesy, A.I.; Abdel-Rahman, A.K.; Bady, M.; Ookawara, S. The Influence of Multi-walled Carbon Nanotubes Additives into Non-edible Biodiesel-diesel Fuel Blend on Diesel Engine Performance and Emissions. *Energy Procedia* **2016**, *100*, 166–172. [CrossRef]
54. Banapurmath, N.R.; Sankaran, R.; Tumbal, A.V.; Hunashyal, A.M.; Ayachit, N.H. Experimental investigation on direct injection diesel engine fuelled with graphene, silver and multiwalled carbon nanotubes-biodiesel blended fuels. *Int. J. Automot. Eng. Technol.* **2014**, *3*, 129–138. [CrossRef]
55. Tewari, P.D.E.; Banapurmath, N.; Yaliwa, V. Experimental investigations on a diesel engine fuelled with multi-walled carbon nanotubes blended biodiesel fuels. *Int. J. Emerg. Technol. Adv. Eng.* **2013**, *3*, 72–76.